Journal of Thermal Analysis and Calorimetry, Vol. 88 (2007) 3, 863–870

EVALUATION OF COMBUSTION CHARACTERISTICS OF DIFFERENT SIZE ELBISTAN LIGNITE BY USING TG/DTG AND DTA

H. Sis[*]

Department of Mining Engineering, Inonu University, 44280 Malatya, Turkey

In this research, the relationship between particle size and combustion kinetics and combustion properties of lignite samples was examined by utilizing the thermogravimetric (TG/DTG) and differential thermal analysis (DTA) techniques. The lignite samples separated into different size fractions were subjected to non-isothermal thermogravimetric analysis between ambient and 900°C in the presence of 50 mL min^{-1} air flow rate. Activation energy (E) and Arrhenius constant (A_r) of combustion reaction of each size was evaluated by applying Arrhenius kinetic model to the resulting data. Combustion properties of the samples were interpreted by careful examination of the curves. The apparent activation energies in major combustion region were calculated as 41.03 and 53.11 kJ mol^{-1} for the largest size (–2360+2000 μm) and the finest size (–38 μm), respectively.

Keywords: *activation energy, combustion, lignite, particle size, thermal analysis*

Introduction

Coal is the source of about 27% of the world primary energy consumption and it accounts for about 34% of all the electricity generated in the world, and much of this occurs by means of the combustion of pulverized coal [1]. The studies on the combustion and pyrolysis behavior of fossil fuels have gained a wide acceptance among researchers in the last decades. One of the main objectives in coal combustion investigations is the development of comprehensive computer models to design combustors and gasifiers for the clean utilization of coal usually in complex burners and combustion chambers [2].

In the coal science field, thermogravimetry (TG), differential scanning calorimetry (DSC), and differential thermal analysis (DTA) techniques have been found useful tools to study the combustion and pyrolysis behavior and kinetics of coals. During coal combustion, different reactions take place and solid, liquid, and gaseous product are formed and mass loss of the sample is recorded with time and temperature by TG instruments. Non-isothermal combustion tests have great advantage of being able to achieve complete conversion of coal and hence characterization of char with a wide range of reactivities in a single run [3]. DTA and DSC instruments are usually employed under identical experimental conditions with TG to track the reaction type (i.e., endothermic or exothermic), to calculate kinetics and heat flow rates, and also to delineate TG/DTG combustion curves.

Researches showed that combustion properties of coal depends on coal rank or type, coal size, and operational parameters such as temperature, heating rate, pressure, and volume of flowing gas [4–9]. Smith *et al.* [10] examined sixty six coals, varied in rank from lignite to low-volatile bituminous, as part of a coal characterization programme. Coal combustion experiments were carried out over the temperature range of 25–900°C using air at atmospheric pressure in a derivative thermogravimetry. They found that combustion rates increased progressively with increasing temperature, passed through maxima and then declined. Milligan *et al.* [9] investigated the combustion profiles of seven different size fractions of coal below 212 μm and concluded that, micronized coal samples showed a greater complexity in their combustion profiles than the larger particle sizes.

Modeling the combustion process of coal is extremely complicated because of its heterogeneity and oxidation of several components simultaneously. A method was developed by Cumming [11] to describe the combustibility of solid fuels, such as lignite, bituminous coals and petroleum coke, in terms of weighted mean apparent activation energy, derived from simultaneous TG/DTG readings with a certain mass of sample heated at a constant rate in flowing air atmosphere. A number of models were proposed for the evaluation of TG data for kinetic purposes e.g., Arrhenius method [8, 12], Coats–Redfern method [13, 14], Freeman–Carrol method [15, 16] and Reich–Stivala method [17, 18]. Arrhenius kinetic model is the most widely used model in the pyrolysis

---

[*] hsis@inonu.edu.tr

1388–6150/$20.00

Akadémiai Kiadó, Budapest, Hungary
Springer, Dordrecht, The Netherlands

and combustion kinetic of coal due to its reliability and simplicity. Kök *et al.* [8] carried out non-isothermal thermogravimetric experiments for twelve different size fractions of the coal sample. TG/DTG experiments were performed from ambient to 900°C in air atmosphere and the data were analyzed using an Arrhenius type reaction model assuming first-order reaction kinetics. Kinetic parameters were calculated and the results were compared and explained in terms of mineral matter composition in different fractions.

The present work focuses on the investigation of the combustion behavior of different size lignite from the same origin. Therefore, the crushed lignite samples were sieved to different size fractions and non-isothermal heating conditions were applied on each size fractions separately. Kinetic analysis of the thermogravimetry data was made by applying Arrhenius kinetic model to calculate the effective equation parameters. The data obtained from DTA experiments were used to monitor the combustion characteristics of lignite and interpret TG/DTG curves.

Experimental

Sample preparation

Lignite, used in this study, was obtained from Elbistan region, the largest lignite source in Turkey. Lignite reserve is 3.4 billion tons and it corresponds to more than the half of the total reserve of the country. The run-of-mine lignite is mainly consumed in Afsin/Elbistan power plant with 4·344 MW capacity. As a low rank coal, in-situ samples contain about 70% moisture. Approximately 100 kg of run-of-mine lignite was picked up from the site and prepared for analysis. The air-dried lignite samples were, first crushed below 20 mm by a jaw crusher followed by reducing the size below 2.5 mm using hammer mill. The crushed lignite was air-dried again and representative samples were taken for proximate, ultimate and thermal analysis.

Proximate analysis of the lignite samples were conducted in accordance with ASTM standards and the results are given in Table 1. Leco CHNS-932, from LECO Corporation, MI, USA, was used for analysis of C, H, N and S elements. It is seen from Table 1 that air-dried coal sample contains high moisture and volatile matter, as 13.48 and 40.80%, respectively, but low fixed carbon, as 20.67%.

The crushed lignite samples were sieved with standard sieve series to obtain 14 different size fractions. Particle size distribution of the sample and the proximate analysis of each size fraction are given in Tables 2 and 3, respectively. The largest and the finest sizes were prepared as –2360+2000 and –38 μm, respectively. When Table 2 is inspected, it can be realized that the wide size range of crushed lignite was divided (or sieved) into 14 narrow size ranges of the samples to achieve more and reliable data. As seen in the Table 3, larger sizes contain more moisture but less ash than finer sizes since the ash-forming minerals, e.g. clay minerals, are naturally fine in size.

Table 1 Proximate and ultimate analysis of Elbistan lignite samples*

Proximate analysis	Mass/%
Moisture	13.48
Ash	25.05
Volatile matter	40.80
Fixed carbon	20.67
Ultimate analysis	**Mass/%**
C	40.51
H	4.38
N	0.68
S	2.67
O (by difference)	13.23

*air-dried basis

Thermal experiments

Non-isothermal thermogravimetric tests of different size materials were carried out by computer-controlled TGA 50 and DTA 50 thermal analyzers from Shimadzu, Japan. Prior to tests, TG instrument was calibrated for temperature readings with indium reference standard and the digital microbalance of the instrument was auto-calibrated for the precise reading of the mass changes of the sample. In DTA, α-alumina was used as the reference material.

The experimental procedure involves placing approximately 10 mg of the sample in a platinum crucible, setting the heating and gas (air) flow rates and then executing the test. For all experiments, heating and air flow rates were kept constant at 10°C min^{-1} and 50 mL min^{-1}, respectively, in the temperature range from ambient to 900°C. The experiments were repeated under identical conditions to check the reproducibility of the results.

Kinetic analysis

The analysis of the kinetic data is based on the following kinetic equation:

$$\frac{\mathrm{d}\alpha}{\mathrm{d}t}=k\alpha^{n} \tag{1}$$

where α is the amount of the sample undergoing the reaction, *n* is the order of reaction, and *k* is the spe-

Table 2 Particle size distribution of Elbistan lignite*

Screen size range (mesh)	Screen size range/ µm	Mass/ g	Mass/ %	Cumulative oversize/%	Cumulative undersize/%
–8+10	–2360+2000	180.224	10.84	10.84	89.16
–10+18	–2000+1000	721.59	43.42	54.26	45.74
–18+20	–1000+850	116.12	6.99	61.25	38.75
–20+30	–850+600	181.088	10.90	72.15	27.85
–30+35	–600+500	75.513	4.54	76.69	23.31
–35+50	–500+300	136.896	8.24	84.93	15.07
–50+70	–300+212	67.184	4.04	88.97	11.03
–70+100	–212+150	52.408	3.15	92.12	7.88
–100+140	–150+106	39.782	2.39	94.51	5.49
–140+200	–106+75	29.975	1.80	96.31	3.69
–200+270	–75+53	24.169	1.46	97.77	2.23
–270+325	–53+45	8.453	0.51	98.28	1.72
–325+400	–45+38	7.812	0.47	98.75	1.25
–400	–38	20.85	1.25	100.00	0.00
total		1662.064	100.00		

* air-dried basis

Table 3 Proximate analysis of Elbistan lignite of different sizes*

Particle size range/µm	Moisture/%	Ash/%	Volatile matter/%	Fixed carbon/%
–2360+2000	15.39	25.52	42.77	16.32
–2000+1000	14.14	24.16	41.55	20.15
–1000+850	14.31	24.45	41.97	19.27
–850+600	15.32	24.92	41.21	18.55
–600+500	15.19	24.88	40.49	19.44
–500+300	15.41	25.47	40.73	18.39
–300+212	14.88	25.73	43.39	16.00
–212+150	14.55	25.88	44.80	14.77
–150+106	14.43	26.14	36.53	22.90
–106+75	14.31	26.53	37.13	22.03
–75+53	13.99	27.45	41.72	16.84
–53+45	13.60	29.09	39.38	17.93
–45+38	13.32	30.15	38.67	17.86
–38	12.04	35.26	39.44	13.26

*air-dried basis

cific rate constant. The temperature dependence of k is expressed by the Arrhenius equation as:

$$k = A_{\mathrm{r}} \exp\left(-\frac{E}{RT}\right) \tag{2}$$

where A_{r} is the Arrhenius constant, E is the activation energy, T is the temperature, and R is the gas constant. Based on the Eq. (1), the rate of mass change with time ($\mathrm{d}W/\mathrm{d}t$) is equal to:

$$\frac{\mathrm{d}W}{\mathrm{d}t} = kW^{\mathrm{n}} \tag{3}$$

Assuming first-order kinetics (n=1) and substituting k into Eq. (1);

$$\frac{\mathrm{d}W}{\mathrm{d}t} = A_{\mathrm{r}} \exp\left(-\frac{E}{RT}\right) W \text{ or} \tag{4}$$

$$\frac{(\mathrm{d}W/\mathrm{d}t)}{W} = A_{\mathrm{r}} \exp\left(-\frac{E}{RT}\right) \tag{5}$$

are obtained. Taking the logarithm of both sides,

$$\log\left(\frac{\mathrm{d}W/\mathrm{d}t}{W}\right) = \log A_{\mathrm{r}} - \frac{E}{2.303RT} \tag{6}$$

when $\log[(dW/dt)/W]$ is plotted *vs*. $1/T$, a straight line is obtained that will give a slope equals to $E/2.303R$ from which activation energy, E, and an intercept equals to $\log A_r$ from which Arrhenius constant, A_r, can be estimated.

Results and discussion

Combustion characteristics of the lignite samples

The non-isothermal thermogravimetric analyses of the samples were performed between ambient temperature and 900ºC in an air atmosphere and the data obtained from several size fractions were given in Fig. 1. The TG curves of coals display differences to some extend due to variation in combustion properties of different sizes and compositions (Table 3). When the mass losses on the combustion profiles are examined for all sizes, three major reaction regions are distinguishable at certain temperature intervals. The first region (or region 1) takes place below 200ºC, the second region (or region 2), ranges from 200°C to about 550ºC, and the third region (or region 3) starts from 550ºC and continues up to 900°C. Regarding mass losses with respect to total sample mass, 11–13 and 8–11% were took place in the region 1 and region 3, respectively, whereas major mass loss (44–56%) occurred in the region 2.

From the Fig. 1, the amount of the residue (presented in Table 4) is also notable as a general increase is observed with the reduction in the particle size which is in accord with proximate analysis given in Table 3.

Normalized DTG curves of the previously given size fractions are plotted in Fig. 2 which exhibit the reaction regions even more clearly. The first region refers to the release of moisture from the samples and shows that the peak temperature, at which the maximum mass loss occurs, vary from 110°C for the largest size fraction (–2360+2000 μm) to 80°C for the finest size (–38 μm). It can be realized that the main moisture loss occurs at higher temperatures for larger sizes that due to the delayed diffusion of the heat inside larger particles.

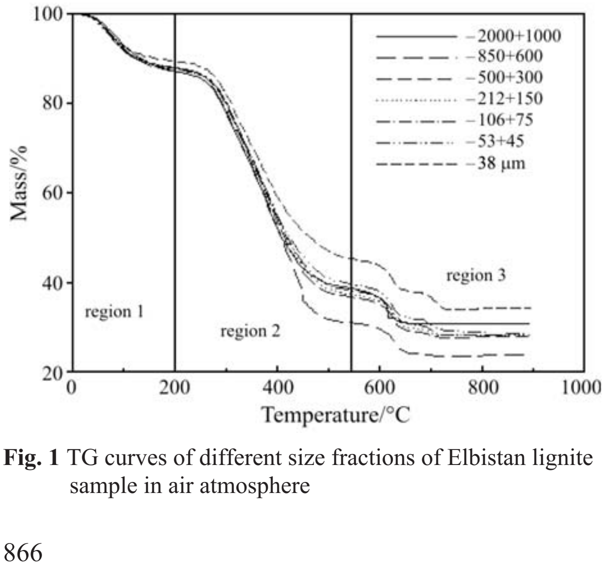

Fig. 1 TG curves of different size fractions of Elbistan lignite sample in air atmosphere

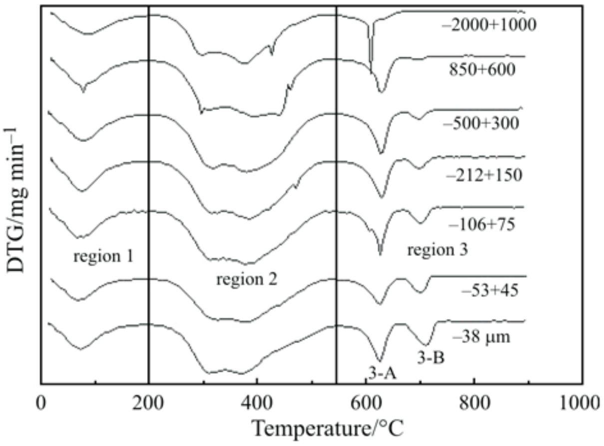

Fig. 2 DTG curves of different size fractions of Elbistan lignite

The second region is the most important region to examine since the major mass loss and complicated chemical reactions, such as formation of liquid and gaseous products, devolatilization, and fixed carbon combustion, occur in this interval. Double peak display seen from DTG profiles is an indication of the stepwise volatile release and the burning of heterogeneous organic matter in the coal samples. Characteristic peak temperature for each size, listed in Table 5, exhibits that despite some fluctuations, the peaks shift slightly to lower temperature value as the particle size decreases. The lower peak temperature could be regarded as the result of higher reactivity of the samples and the reason should be explained in terms of increased surface area with reduced sizes that results in more interaction between air (oxygen) and carbon surfaces and hence early start of ignition. This result is supported by other investigators. For instance, working on the thermogravimetry of different size coals, Shah and Ahmed [19] found reduction of particle size advantageous as it decreased the ignition temperature. Some controversial results were also declared in the literature. Morgan *et al.* [6] observed that for larger particles the commencement of devolatilization was delayed, with a distinct volatiles release at sizes larger than 63 μm, however they could not find a trend in the combustion profiles with increasing initial particle size. Additionally, Milligan *et al.* [9] postulated that the TG and DTA peaks increases in magnitude with increasing particle size above 38–75 μm coal fraction and the heat released from the combustion of the volatiles allowed earlier ignition of the char. The reason for the discrepancy should be explained in terms of differences in type, rank, and origin of coals.

Table 4 Residue amount and burn-out temperature of different size fractions of the lignite sample

Particle size range/μm	Residue mass/%	Burn-out temp./°C
–2360+2000	25.76	633.86
–2000+1000	30.87	666.38
–1000+850	21.33	722.15
–850+600	23.87	711.80
–600+500	28.10	756.47
–500+300	28.10	723.24
–300+212	28.52	729.92
–212+150	28.43	728.96
–150+106	28.14	722.51
–106+75	28.82	723.76
–75+53	30.01	727.62
–53+45	30.66	719.74
–45+38	31.71	725.04
–38	34.41	726.66

The third region corresponds mainly to the decomposition of mineral matter in lignite, such as quartz, kaolinite, montmorillonite and calcite [13]. They start decomposing at temperatures from 600–650°C up to 800–850°C and 8–11% of the total mass was combusted in this range [20]. When the region is scrutinized it is seen that number of peaks is one for larger sizes (i.e., –2360+2000 and –2000+1000 μm), whereas it is two for finer sizes. The region 3 was subdivided into two regions, named regions 3-A and 3-B, for the samples exhibiting two peaks. The temperature values for the first peaks in region 3-A are very close and vary between 616 and 629°C without any order. But, when the second peaks in region 3-B are examined a slight increase of temperature is observed for finer sizes since the peaks seen at 692 and 711°C belong to –850+600 and –38 μm size fractions, respectively.

Burn-out temperatures, after which no further mass loss occurs, were also detected from the third region of DTG profiles and listed in Table 4. A general increase in burn-out temperature was observed in the range of 633–727°C as the particle size decreased from –2360+2000 to –38 μm. A close relationship between peak and burn-out temperatures can be inferred from the data as both of them increase with reduced sizes. The result could be explained by the differences in composition of different sizes. Mineral matters, for example carbonates and pyrite, exist more in finer size than larger size of coal (Table 3). The more is the mineral matter, the more is decomposition which, in turn, yields in higher burn-out and peak temperatures.

DTA experiments, carried out under identical conditions with TG/DTG runs, were plotted in Fig. 3 which shows three major reaction regions similar to Fig. 2. Region 1 (T<200°C) represents endothermic reaction where the heat is being absorbed by the samples while losing moisture. Thermal reactions took place during combustion can be explained well when Figs 2 and 3 are examined together. The exothermic reactions, displayed by two or more peaks in the second region of the both figures, were attributed to the stepwise volatile release and the burning of heterogeneous organic matter in the coal samples, as explained before. DTA curves for all samples have similar patterns since the peaks in the region 2 shifts to lower temperatures as particle size decreases. The reason was explained by the increased surface area with reduced sizes that leads to ignition and combustion of the samples more easily. In the third region, exothermal effects are exhibited by peaks having different magnitude and shape. Intense and narrow peaks were observed for larger sizes, whereas shallow and broad peaks were noticed for finer sizes. The reason is attributable to the difference between the decomposition nature of mineral matter and char. Mineral matter, found more in finer sizes than larger sizes, decomposes slower than char under specified conditions which, in turn, results in broader peaks.

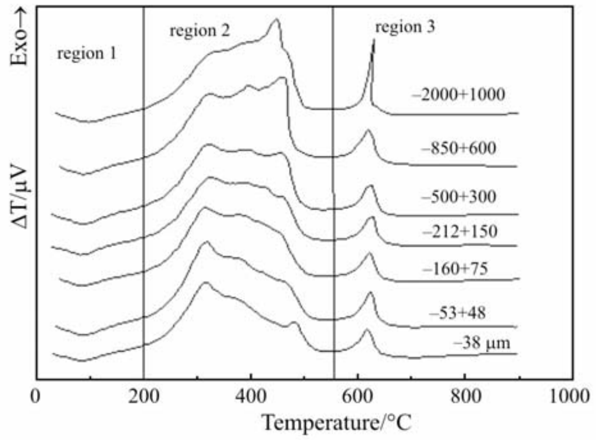

Fig. 3 DTA curves of Elbistan lignite samples with different sizes

Kinetic analysis results

Instead of estimation of the overall kinetic parameters for the whole TG/DTG profile, it is more convenient to apply Arrhenius kinetic, Eq. (6), separately for the three regions described. The kinetic model was applied accordingly, as illustrated in Fig. 4, for randomly selected sizes and the equation parameters are tabulated in Table 5.

The first region is the low temperature region (T<200°C) where the mass loss is mainly due to the removal of moisture in lignite. Concerning activation energy (E), it varied slightly between 32.91 and

Table 5 Kinetic parameters calculated from TG and DTG curves for different size fractions of Elbistan lignite

Particle size range/μm	Reaction region 1 (ambient–200°C)			Reaction region 2 (200–550°C)		
	E/kJ mol^{-1}	A_r/s^{-1}	peak temp./°C	E/kJ mol^{-1}	A_r/s^{-1}	peak temp./°C
–2360+2000	41.38	211.15	108.08	41.03	1.69	386.74
–2000+1000	34.38	40.20	83.14	47.77	7.73	375.24
–1000+850	33.55	32.70	85.58	44.23	0.50	407.64
–850+600	33.20	31.56	79.96	39.62	1.25	391.94
–600+500	36.71	111.43	80.1	45.69	4.07	390.86
–500+300	33.29	31.92	79.37	48.20	7.61	382.07
–300+212	36.65	36.65	78.92	58.45	78.25	381.35
–212+150	38.71	38.71	76.47	48.24	7.48	385.32
–150+106	37.74	37.74	78.07	49.82	10.81	385.14
–106+75	32.97	32.97	74.80	51.37	14.48	381.54
–75+53	32.91	32.91	79.56	50.74	13.16	377.03
–53+45	34.06	34.06	75.7	51.49	14.77	376.06
–45+38	40.28	40.28	67.73	50.33	11.30	375.91
–38	38.95	38.95	68.79	53.11	19.85	370.30

Particle size range/μm	Reaction region 3-A (550–640°C)			Reaction region 3-B (640–900°C)		
	E/kJ mol^{-1}	A_r/s^{-1}	peak temp./°C	E/kJ mol^{-1}	A_r/s^{-1}	peak temp./°C
–2360+2000	151.20	$5.2\cdot10^{6}$	624.21	N/A	N/A	N/A
–2000+1000	178.12	$2.1\cdot10^{7}$	616.02	N/A	N/A	N/A
–1000+850	206.12	$1\cdot10^{10}$	622.06	376.71	$3.8\cdot10^{16}$	702.25
–850+600	68.70	$3.1\cdot10^{8}$	631.36	278.0	$1.1\cdot10^{11}$	692.27
–600+500	172.43	$6\cdot10^{6}$	628.41	387.62	$1.4\cdot10^{17}$	696.05
–500+300	188.12	$6.3\cdot10^{8}$	627.80	470.77	$5.4\cdot10^{21}$	697.07
–300+212	208.85	$1.0\cdot10^{10}$	628.60	564.11	$7.8\cdot10^{26}$	699.72
–212+150	197.66	$2.2\cdot10^{9}$	628.66	517.20	$2.7\cdot10^{24}$	696.37
–150+106	180.03	$2.0\cdot10^{8}$	628.44	485.55	$6.2\cdot10^{22}$	697.86
–106+75	187.94	$6.2\cdot10^{8}$	627.32	562.20	$8.7\cdot10^{26}$	700.89
–75+53	205.81	$7.0\cdot10^{9}$	627.51	501.24	$3.2\cdot10^{23}$	706.24
–53+45	184.09	$3.4\cdot10^{8}$	627.67	472.80	$1.4\cdot10^{22}$	705.37
–45+38	189.15	$6.3\cdot10^{8}$	626.93	531.17	$1.8\cdot10^{25}$	704.58
–38	200.74	$2.9\cdot10^{9}$	625.55	422.49	$3.4\cdot10^{19}$	710.64

41.38 kJ mol^{-1}, but no a certain trend was observed for different sizes in this region.

Concerning the essential reaction region (region 2), apparent activation energies were calculated for all fractions and found 41.03 and 53.11 kJ mol^{-1} for the largest (–2360+2000 μm) and finest (–38 μm) sizes, respectively. Even though some variations were observed, activation energies generally increased slightly with decreasing particle size. Our findings were confirmed by previous studies conducted by Kök *et al.* [8] and Ozbas *et al.* [21] worked on the combustion of different size lignite samples. The reason can be explained by different composition of the size fractions since higher mineral matter content makes coal less prone to ignition and burning which leads to higher E. Additionally, agglomeration of finer particles may occur due to the development of thermoplasticity in this temperature range that increases activation energy.

When the third region is compared with the first and second regions, a tremendous rise is observed in activation energies as the values jump to as high as 208.85 and 564.11 kJ mol^{-1} for the region 3-A and region 3-B, respectively. Recently, Kök *et al.* [22] investigated the combustion properties of various lignite samples from different origins and evaluated the

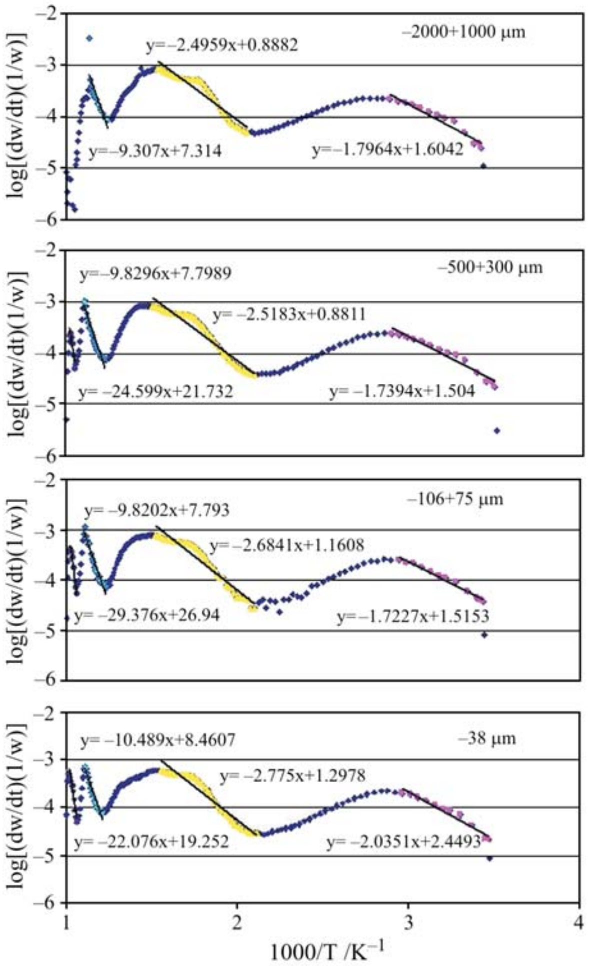

Fig. 4 Determination of kinetic parameters by applying Arrhenius kinetic model (Eq. (6)) to thermogravimetric data curves

three reaction regions separately. They found much higher activation energies in the region 3 than regions 1 and 2. The overall activation energy in region 3 was calculated as 273.5 and 274.8 kJ mol^{-1} for Celtek and Elbistan lignites, respectively. The reason behind this phenomenon is the decomposition difficulty and less reactivity of mineral matter with respect to char found mostly in the region 2.

Conclusions

TG/DTG and DTA curves revealed three major reaction regions at certain temperature intervals. The characteristic peak temperatures, combustion kinetics and reaction type were evaluated separately for each region on the curves and for each sample size and the following conclusions were drawn.

- When the peak temperatures were considered in the region 1, it was seen that moisture loss occurred at higher temperatures for larger particle sizes. The reason was explained by delayed diffusion of the heat inside larger particles.
- TG/DTG curves in the region 2 exhibited that characteristic peaks shifted slightly to lower temperatures as the particle size decreased. It was argued that reduction of particle size increased total surface area of the sample that results in more interaction between air (oxygen) and carbon surfaces and hence early start of ignition.
- When burn-out and peak temperatures were evaluated in region 3, a slight increase was observed for finer sizes. It was attributed to the differences in mineral matter contents of different sizes as finer sizes contain more mineral matter than larger size of coal.
- DTA curves displayed one endothermic peak in the region 1 for all the samples denoted the moisture release from the samples. Two or three exothermic peaks aroused in region 2 were attributed to the stepwise volatile release and the burning of heterogeneous organic matter in the coal samples. The exothermic peak in the region 3 resulted from the decomposition of mineral matter in the samples.
- For the essential reaction region (region 2), apparent activation energies were calculated for all fractions and found 41.03 and 53.11 kJ mol^{-1} for the largest and the finest sizes, respectively. Activation energies slightly increased with decreasing particle size. Furthermore, the activation energies jumped to as high as 564 kJ mol^{-1} in region 3-B. The reason was attributed to the decomposition difficulty and less reactivity of mineral matter with respect to char.

References

1 A. Williams, R. I. Backreedy, R. Habib, J. M. Jones and M. Pourkashanian, Fuel, 81 (2002) 605.
2 R. I. Backreedy, R. Habib, J. M. Jones, M. Pourkashanian and A. Williams, Fuel, 78 (1999) 1745.
3 L. G. Tang, R. P. Gupta, C. D. Sheng and T. F. Wall, Fuel 84 (2005) 127.
4 K. E. Benfell, B. B. Beamish and K. A. Rodgers, Thermochim. Acta, 298 (1997) 119.
5 K. E. Benfell, B. B. Beamish, P. J. Crosdale and K. A. Rodgers, Fuel Process. Technol., 60 (1999) 1.
6 P. A. Morgan, S. D. Robertson and J. F. Unsworth, Fuel, 65 (1986) 1546.
7 S. A. Jayaweera, J. M. Moss and M. W. Thwaites, Thermochim. Acta, 152 (1989) 215.
8 M. V. Kök, E. Ozbas, C. Hicyilmaz and O. Karacan, Thermochim. Acta, 302 (1997) 125.
9 J. B. Milligan, K. M. Thomas and J. C. Crelling, Fuel, 76 (1997) 1249.
10 S. E. Smith, R. C. Neavel, E. J. Hippo and R. N. Miller, Fuel, 60 (1981) 458.
11 J. W. Cumming, Fuel, 63 (1984) 1436.
12 K. E. Ozbas, M. V. Kök and C. Hicyilmaz, J. Therm. Anal. Cal., 69 (2002) 541.

13 I. Y. Elbeyli and S. Piskin, J. Therm. Anal. Cal., 83 (2005) 721.
14 D. Borah, M. Barua and M. K. Baruah, Fuel Process. Technol., 86 (2005) 977.
15 R. W. Mickelson and I. N. Einhorn, Thermochim. Acta, 1 (1970) 147.
16 K. Rajeshwar, Thermochim. Acta, 45 (1981) 253.
17 E. House, Thermochim. Acta, 57 (1982) 47.
18 L. Reich and S. S. Stivala, Thermochim. Acta, 24 (1978) 9.
19 M. R. Shah and N. Ahmed, Fuel Sci. Technol. Int., 12 (1994) 85.
20 J. V. O'Gorman and P. L. Walker, Fuel, 52 (1973) 71.
21 K. E. Ozbas, C. Hicyilmaz, M. V. Kök and S. Bilgen, Fuel Process. Technol., 64 (2000) 211.
22 M. V. Kök, G. Pokol, C. Keskin, J. Madarász and S. Bagci, J. Therm. Anal. Cal., 76 (2004) 247.

Received: November 10, 2005
Accepted: February 8, 2006
OnlineFirst: August 11, 2006

DOI: 10.1007/s10973-005-7447-4